Journal of Molecular Graphics and Modelling 48 (2014) 60–69

Contents lists available at ScienceDirect

Journal of Molecular Graphics and Modelling

journal homepage: www.elsevier.com/locate/JMGM

Mechanism, kinetics and atmospheric fate of $CF_3CH{=}CH_2$, $CF_3CF{=}CH_2$, and $CF_3CF{=}CF_2$ by its reaction with OH-radicals: CVT/SCT/ISPE and hybrid meta-DFT methods

Balaganesh M., Rajakumar B.*

Department of Chemistry, Indian Institute of Technology Madras, Chennai 600036, India

ARTICLE INFO

Article history:
Received 26 September 2013
Received in revised form
30 November 2013
Accepted 2 December 2013
Available online 11 December 2013

Keywords:
Dual level
CVT/SCT/ISPE
HFOs
Lifetime
Radiative forcing
GWP

ABSTRACT

The dual level direct dynamic study is carried out for the reactions of $CF_3CH{=}CH_2$, $CF_3CF{=}CH_2$ and $CF_3CF{=}CF_2$ with hydroxyl radicals. The dynamic calculations are performed using the variational transition state theory (VTST) with interpolated single-point energies (ISPE) method at M06-2X/MG3S//M06-2X/6-31+G(d,p) level of theory. All the possible reactions such as abstraction and addition–elimination pathways are explored for the title reactions. The temperature dependent rate coefficients using canonical variational transition state theory with small curvature tunneling for the reaction of OH radicals with test molecules over the temperature range of 200–3000 K are computed. The predicted rate coefficients (in 10^{-12} cm^3 $molecule^{-1}$ s^{-1}) using CVT/SCT/ISPE methodology for the reaction of $CF_3CH{=}CH_2$, $CF_3CF{=}CH_2$ and $CF_3CF{=}CF_2$ with OH radicals are 1.48, 1.02 and 1.77, respectively, are in good agreement with reported ones at 298 K. The atmospheric lifetimes for the test molecules $CF_3CH{=}CH_2$, $CF_3CF{=}CH_2$ and $CF_3CF{=}CF_2$ are calculated at 277 K to be 8, 11 and 6 days, respectively. Global warming potentials are also reported for the different time horizon of 20, 100 and 500 years.

1. Introduction

Chlorofluorocarbons (CFCs) and hydro-chlorofluorocarbons (HCFCs) are major anthropogenic sources of reactive chlorine which initiates ozone destructive cycle in the stratosphere. Recognition of the adverse environmental impact of CFCs release into the atmosphere [1] has led to an effort to replace these compounds with environmentally acceptable alternatives. Chlorine-free, partially fluorinated hydrocarbons (hydro-fluorocarbons or HFCs) have been among the leading ozone-friendly substitutes for CFCs originally targeted under the Montreal Protocol. In general, fluorination of hydrocarbons reacts a bit slower toward tropospheric OH, thus increasing their residence time in the atmosphere to a few decades and even hundreds of years. Fully fluorinated alkanes do not react with OH, and their atmospheric lifetimes are estimated to be as long as thousands of years [2]. Hydrofluoro-olefins (HFOs) are currently under consideration as potential environmental friendly CFCs substitutes. The presence of a carbon–carbon double bond is expected to render these substances highly reactive toward the hydroxyl radical resulting in an optimally short tropospheric lifetime, thereby limiting their accumulation in the atmosphere and minimizing their direct global warming potentials (GWPs). Also fluorinated alkenes are widely used in chemical industry as starting materials in syntheses of various halogenated compounds, fluoropolymer and fire suppressing, cleaning, and etching agents. So, extensive studies on these compounds will be helpful in reliable atmospheric modeling.

The atmospheric and kinetic studies for the test molecules were investigated by several research groups with various experimental techniques. Orkin et al. [3–5] studied the reaction of OH radicals with $CF_3CH{=}CH_2$, $CF_3CF{=}CH_2$ and $CF_3CF{=}CF_2$ using flash photolysis resonance fluorescence technique in the temperature range of 252–370 K. Sulbaek Andersen et al. [6] used long-path length FT-IR smog chamber techniques to study the OH + $CF_3CH{=}CH_2$ reaction in 700 Torr of N_2 diluents at 296 K. Thomsen and Jorgensen [7] studied addition reaction of OH radical with $CF_3CH{=}CH_2$ using DFT, MP2 and CCSD(T) methods and they have reported the rate coefficient at 298 K. They concluded that, computed rate constants using MP2/cc-pVTZ//BH&HLYP/cc-pVTZ level of theory are in good agreement with experimental values. Recently, Zhang et al. [8] studied the detailed mechanism for the reaction of $CF_3CH{=}CH_2$ with OH radicals, which were performed at the MP2 and BMC-CCSD levels of theory. They have reported the rate coefficients for this reaction in the temperature range of 200–3000 K using RRKM theory. However, the trend of the rate coefficients was quite opposite (with a strong positive temperature dependence) to that of the experimentally measured ones.

* Corresponding author. Tel.: +91 4422574231; fax: +91 4422574202.
E-mail addresses: rajakumar@iitm.ac.in, ballarajakumar@gmail.com (R. B.).

1093-3263/$ – see front matter © 2014 Elsevier Inc. All rights reserved.
http://dx.doi.org/10.1016/j.jmgm.2013.12.003

Gas phase reaction of OH radical with $CF_3CF{=}CH_2$ was studied by Nielsen et al. [9] using long path length FTIR-smog chamber technique in 700 Torr of N_2, N_2/O_2, or air diluents at 296 K. Papadimitriou et al. [10] studied this reaction using pulsed laser photolysis/laser induced fluorescence technique over the temperature range of 206–380 K. Du et al. [11] studied the possible reaction mechanism for the reaction of OH radicals with $CF_3CF{=}CH_2$ using CCSD(T)/6-311++G(d,p)//MP2(full)/6-311++G(d,p) level of theory in the temperature range of 206–380 K. The reported rate coefficients by Du et al. [11] seem to be lower than the experimentally measured ones.

The kinetic study of OH + $CF_3CF{=}CF_2$ reaction was carried out experimentally by several research groups. Tokuhashi et al. [12] studied this reaction using flash photolysis and laser photolysis method combined with laser induced fluorescence technique in the temperature range of 250–430 K. Mashino et al. [13] used FTIR-smog chamber technique to study this reaction at 296 K; and CF_3CFO and FCFO were reported to be the major products. Acerboni et al. [14] used long-path FTIR detection technique to study this reaction at 298 K. CF_3CFO and FCFO were found to be major products in their investigation. McIlroy and Tully [15] studied this reaction over the temperature range of 293–831 K using pulsed laser photolysis/laser induced fluorescence technique. Dubey et al. [16] used discharge flow combined with resonance fluorescence technique to study the OH + $CF_3CF{=}CF_2$ reaction over the temperature range of 249–296 K. Even though, number of experimental studies on OH + $CF_3CF{=}CF_2$ reaction are available, no theoretical study is reported so far to understand the mechanistic aspects, to the best of our knowledge.

As discussed above, there are number of experimental and theoretical studies available on the title reactions till now. However, no detailed mechanistic investigations (such as the contribution from abstraction and addition channels) on the title reactions are reported so far in the literature, to the best of our knowledge. In case of all the three reactions, no theoretical reports on radiative forcing and global warming potentials are available so far. We report a wide temperature's range (lower to higher viz., 200–3000 K) rate coefficients in this article. The lower temperature rate coefficients are useful in atmospheric chemistry of these compounds where as the high temperature rate coefficients are interested in pyrolysis and combustion modeling. Also in this article we present detailed reaction mechanisms, atmospheric lifetimes and global warming potentials of the test molecules.

$$CH_3CH{=}CH_2 + OH \xrightarrow{k_1} \text{Products} \quad (1)$$

$$CF_3CF{=}CH_2 + OH \xrightarrow{k_2} \text{Products} \quad (2)$$

$$CF_3CF{=}CF_2 + OH \xrightarrow{k_3} \text{Products} \quad (3)$$

2. Computational methods

The equilibrium geometries of the reactants ($CF_3CH{=}CH_2$, $CF_3CF{=}CH_2$, $CF_3CF{=}CF_2$ and OH), van der Waals complexes (vdWs), transition states (TSs), adducts (ADTs) and products of the abstraction and addition reactions were optimized at M06-2X/6-31+G(d,p) level of theory [17–19]. Harmonic vibrational frequencies for all the stationary points located on potential energy surface were obtained from optimized geometries using M06-2X/6-31+G(d,p) level of theory. It should be noted that the performance of this functional is tested against diverse database by Truhlar and co-worker [17]. They have concluded that M06-2X functional is good for main-group thermo chemistry, kinetics and also for the prediction of non-covalent interactions. The error which is predicted by M06-2X functional is lesser than B98 functional which in turn lesser than B3LYP functional [17,18]. All the reactants, ADTs and products were recognized with zero imaginary frequency and TSs were recognized with one imaginary frequency. Intrinsic reaction coordinate (IRC) [20] calculations were performed to verify the designated transition states connect the reactants and products. To improve the accuracy of the calculated reaction energy, the single-point energy calculations were carried out for all the stationary points at M06-2X functional with MG3S (modified Gaussian-3 semidiffuse) basis set. The scaled harmonic vibrational frequencies [21] were used in dynamic calculations. The theoretical rate coefficients were calculated using canonical variational transition state theory (CVT) [22–24] with small-curvature tunneling (SCT) [25,26] by employing the POLYRATE 2008 program [27] and GAUSSRATE 2009A [28] for the title reactions at M06-2X/6-31+G(d,p) theory. All the electronic structure calculations were carried out using Gaussian 09 [29] and normal modes of stationary points are viewed in Gauss View [30].

3. Results and discussion

Reactions of OH radicals with $CF_3CH{=}CH_2$, $CF_3CF{=}CH_2$ and $CF_3CF{=}CF_2$ undergo various pathways together with abstraction and addition–elimination channels. All these channels are initiated from the weakly bound van der Waals complex which is formed by the approach of OH radical to electron deficient ⟩C=C⟨ bond of $CF_3CH{=}CH_2$, $CF_3CF{=}CH_2$ and $CF_3CF{=}CF_2$. To avoid confusion in the labels of each stationary points along the potential energy surface, we added suffixes a, b and c with all labels for reactions of OH radicals with $CF_3CH{=}CH_2$, $CF_3CF{=}CH_2$ and $CF_3CF{=}CF_2$, respectively. The optimized geometries of all the stationary points along the potential energy surface are shown in SI (Fig. S-V-1). The energy level diagrams for the major pathways in title reactions based on the energies predicted at M06-2X/MG3S//M06-2X/6-31+G(d,p) level are shown in Fig. 1. The complete energy level diagrams for the title reactions are shown in SI (Fig. S-V-2).

3.1. Reaction of OH + $CF_3CH{=}CH_2$

3.1.1. H and F-abstraction pathways

The H atom abstraction reaction pathways of OH radical with $CF_3CH{=}CH_2$ go through the three different channels via transition states TS1a, TS2a and TS3a. TS1a corresponds to the H atom abstraction from —CH= site. TS2a and TS3a correspond to the abstraction from terminal $=CH_2$ group. Unless stated, the energies which are mentioned within the parentheses are zero point corrected and relative to reactant's energies. The products $CF_3C^{\bullet}{=}CH_2$ (−5.35 kcal/mol), $CF_3CH{=}{}^{\bullet}CH$ (−5.85 kcal/mol) and $CF_3CH{=}{}^{\bullet}CH$ (−6.10 kcal/mol) are formed through transition states TS1a (5.25 kcal/mol), TS2a (5.51 kcal/mol) and TS3a (5.52 kcal/mol), respectively. The F atom of CF_3 group can also be abstracted by OH radicals via TS4a with larger barrier height (77.2 kcal/mol).

3.1.2. Addition pathways

The addition pathways are initiated via the weakly bound van der Waals complex (vdWa) lying below the reactant's energy about 3.16 kcal/mol. The electrophilic addition of OH radical on ⟩C=C⟨ bond present in the reactant leads to the stable adducts named ADT1a and ADT2a (−29.3 and −31.2 kcal/mol) via TS5a and TS6a (0.48 and 0.70 kcal/mol), respectively. TS5a and TS6a are the transition states for the addition of OH at terminal and middle carbon atoms of the ⟩C=C⟨ bond, respectively.

3.1.3. Isomerization and dissociation pathways

The ADT1a will undergo isomerization leading to ADT3a (−26.7 kcal/mol) and ADT5a (−37.2 kcal/mol) via four membered ring TS8a (4.95 kcal/mol) by transfer of hydroxyl hydrogen to the

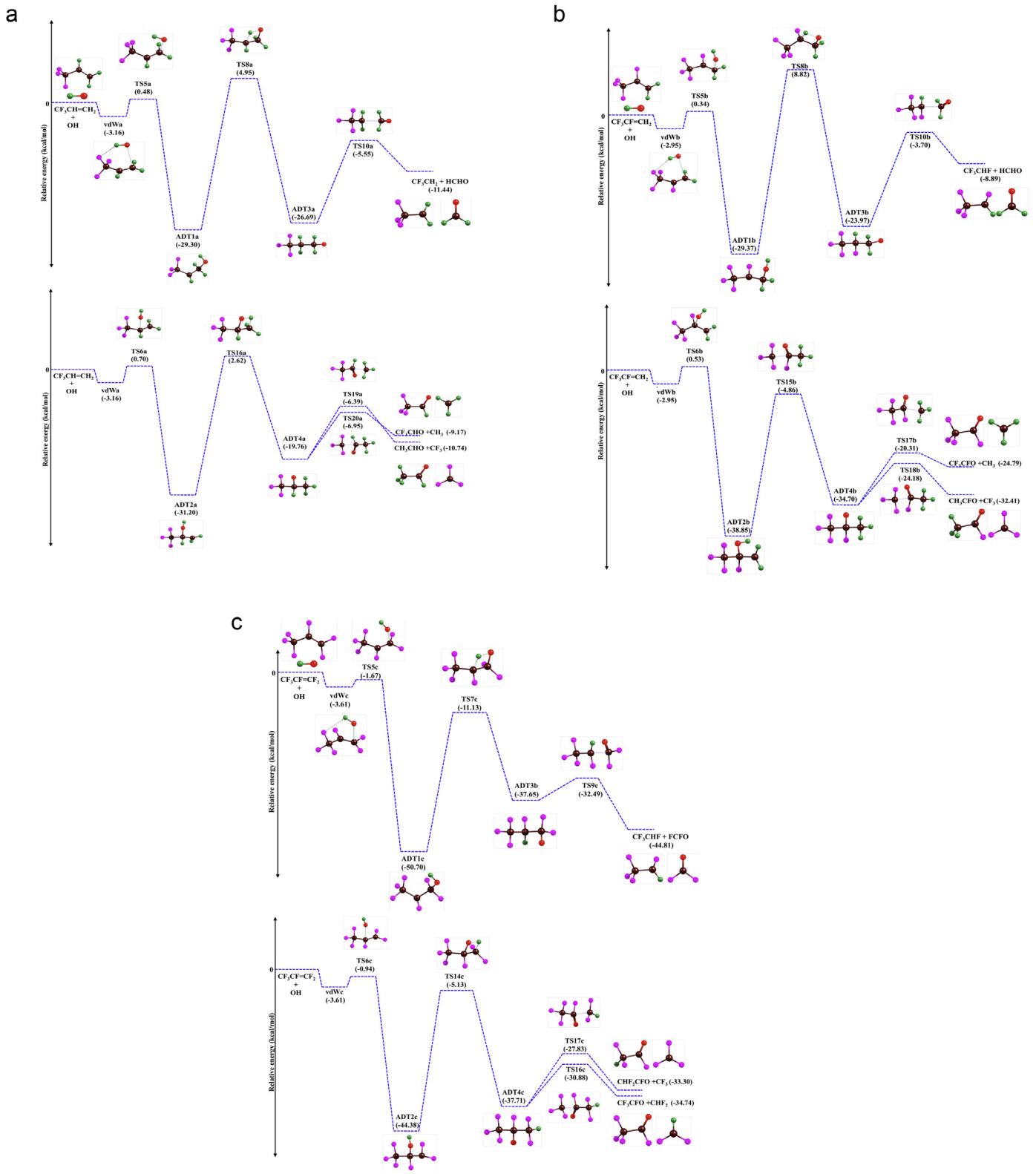

Fig. 1. Barrier heights (kcal/mol) calculated for the potential energy surface of the reactions of OH radical with CF_3—CH=CH_2, CF_3—CF=CH_2 and CF_3—CF=CF_2 at the M06-2X/MG3S//M06-2X/6-31+G(d,p) + ZPE level. Pink, brown, green and red represent fluorine, carbon, hydrogen and oxygen atoms in the structures, respectively. (a) Energy profile for the reaction of OH + CF_3CH=CH_2. (b) Energy profile for the reaction of OH + CF_3CF=CH_2. (c) Energy profile for the reaction of OH + CF_3CF=CF_2.

middle carbon and TS9a (8.16 kcal/mol) by transfer of hydrogen which is attached with terminal carbon to the middle carbon, respectively. Also the ADT1a will undergo terminal C—H cleavage via TS7a to form CF_3CH=CH (OH) + H (−1.27 kcal/mol). ADT3a will undergo C—C bond (which is originated from)C=C(bond) cleavage via TS10a (−5.55 kcal/mol) and C—H bond cleavage at terminal carbon via TS11a (−1.71 kcal/mol) to yield bi-products HCHO + CF_3•CH_2 (−11.5 kcal/mol) and H + CF_3CH_2CHO (−7.77 kcal/mol), respectively. ADT5a yields the bi-products CF_3 + CH_2=CH (OH) (−8.96 kcal/mol) via TS12a (−1.75 kcal/mol)

by CF_3—C cleavage and H + CF_3CH_2CHO (−7.77 kcal/mol) via TS13a (2.33 kcal/mol) by O—H cleavage.

In a similar way that of ADT1a, the ADT2a will undergo isomerization leading to ADT4a (−19.76 kcal/mol) and ADT6a (−37.98 kcal/mol) via four membered ring TS16a (2.62 kcal/mol) by transfer of hydroxyl hydrogen to the terminal carbon and TS17a (7.39 kcal/mol) by transfer of hydrogen which is attached with middle carbon to terminal the carbon, respectively. Also the ADT2a will undergo CF_3—C cleavage via TS14a (0.53 kcal/mol) to form CF_3 + CH_2=CH (OH) (−1.92 kcal/mol) and middle C—H bond cleavage via TS15a (7.32 kcal/mol) to form CF_3C (OH)=CH_2 + H (0.09 kcal/mol). The ADT4a will undergo (i) middle C—H bond cleavage via TS18a (−1.21 kcal/mol) to yield bi-products CF_3COCH_3 + H (−8.14 kcal/mol), (ii) CF_3—C bond cleavage via TS19a (−6.39 kcal/mol) to yield bi-products CH_3CHO + CF_3 (−10.75 kcal/mol) and (iii) CH_3—C bond cleavage via TS20a (−6.95 kcal/mol) to yield bi-products CF_3CHO + CH_3 (−9.17 kcal/mol), respectively. ADT6a yields the bi-products CF_3COCH_3 + H (−8.14 kcal/mol) via TS21a (2.03 kcal/mol) by O—H bond cleavage.

The energy profile for the reaction of OH + CF_3CH=CH_2 is given in SI (Fig. S-V-1a). The pathways forming HCHO and CF_3CHO were found to be the lowest energy and feasible channels when compared to the other product as demonstrated from experimental observations [31].

3.2. Reaction of OH + CF_3CF=CH_2

3.2.1. H and F-abstraction pathways

The H atom abstraction reaction pathways of OH radical with CF_3CF=CH_2 goes through the two different channels via transition states TS1b and TS2b. TS1b and TS2b correspond to the abstraction from terminal =CH_2 group. The products CF_3CF=•CH + H_2O (−2.29 kcal/mol), and CF_3CF=•CH + H_2O (−2.63 kcal/mol) are formed through transition states TS1b (7.99 kcal/mol), and TS2b (6.84 kcal/mol), respectively. Similarly the F atom can be abstracted from —CF_3 and —CF= groups via high barrier transition states TS3b (78.92 kcal/mol) and TS4b (84.32 kcal/mol), respectively, to form the corresponding products.

3.2.2. Addition pathways

The addition pathways are initiated from the weakly bound van der Waals complex (vdWb). The stabilization energy of vdWb is 2.95 kcal/mol compared to reactant's energy. The electrophilic addition of OH radical on ⟩C=C⟨ bond present in the reactant leads to the stable adducts named ADT1b and ADT2b (−29.37 and −38.85 kcal/mol) via TS5b and TS6b (0.34 and 0.53 kcal/mol), respectively. TS5b and TS6b are the transition states for the addition of OH at terminal and middle carbon atoms of the ⟩C=C⟨ bond.

3.2.3. Isomerization and dissociation pathways

The ADT1b will undergo isomerization leading to ADT3b (−23.97 kcal/mol) and ADT5b (−36.39 kcal/mol) via four membered ring TS8b (8.82 kcal/mol) by transfer of hydroxyl hydrogen to the middle carbon and TS9b (14.68 kcal/mol) by transfer of hydrogen which is attached with terminal carbon to the middle carbon, respectively. Also the ADT1b will undergo terminal C—H cleavage via TS7b (7.07 kcal/mol) to form CF_3CF=CH (OH) + H (3.05 kcal/mol). ADT3b will undergo C—C bond (which is originated from ⟩C=C⟨ bond) cleavage via TS10b (−3.70 kcal/mol) and C—H bond cleavage at terminal carbon via TS11b (4.41 kcal/mol) to yield bi-products HCHO + CF_3•CHF (−8.89 kcal/mol) and H + $CF_3CHFCHO$ (−1.58 kcal/mol), respectively. ADT5b yields bi-products CF_3 + CHF=CH (OH) (−1.47 kcal/mol) via TS12b (−0.95 kcal/mol) by CF_3—C cleavage and H + $CF_3CHFCHO$ (−1.58 kcal/mol) via TS13b (8.86 kcal/mol) by O—H cleavage.

The ADT2b will undergo isomerization leading to ADT4b (−34.70 kcal/mol) and ADT6b (−36.04 kcal/mol) via four membered ring TS15b (−4.86 kcal/mol) by transfer of hydroxyl hydrogen to the terminal carbon and TS16b (−7.74 kcal/mol) by transfer of hydrogen which is attached with middle carbon to terminal carbon, respectively. Also the ADT2b will undergo CF_3—C cleavage via TS14b (−5.11 kcal/mol) to form CF_3 + CF(OH)=CH_2 (−5.06 kcal/mol). The ADT4b will undergo (i) CH_3—C bond cleavage via TS17b (−20.31 kcal/mol) to yield bi-products CF_3CFO + CH_3 (−24.79 kcal/mol), (ii) CF_3—C bond cleavage via TS18b (−24.18 kcal/mol) to yield bi-products CH_3CFO + CF_3 (−32.41 kcal/mol) and (iii) middle C-F bond cleavage via TS19b (4.06 kcal/mol) to yield bi-products CF_3COCH_3 + F (4.38 kcal/mol), respectively. ADT6b yields the bi-products CF_3COCH_2F + H (0.11 kcal/mol) via TS20b (8.89 kcal/mol) by O—H bond cleavage.

The energy profile for the reaction of OH + CF_3CF=CH_2 is given in SI (Fig. S-V-1b). The lowest energy pathway on potential energy surface leads to the formation of HCHO and CF_3CFO which are feasible products as expected from experimental studies [32].

3.3. Reaction of OH + CF_3CF=CF_2

3.3.1. F-abstraction pathways

The F atom abstraction reaction pathways of OH radical with CF_3CF=CF_2 goes through the four different channels via high barrier transition states TS1c, TS2c, TS3c and TS4c. The F atom is abstracted from —CF_3, —CF= and =CF_2 groups via TS1c (78.57 kcal/mol), TS3c (82.06 kcal/mol), TS2c (89.50 kcal/mol) and TS4c (89.09 kcal/mol), respectively, to form the corresponding products.

3.3.2. Addition pathways

The weakly bound van der Waals complex vdWc (−3.16 kcal/mol) is formed before it undergoes addition on ⟩C=C⟨ bond of the test molecule. The electrophilic addition of OH radical on ⟩C=C⟨ bond present in the reactant leads to the stable adducts named ADT1c and ADT2c (−50.70 and −44.38 kcal/mol) via TS5c and TS6c (−1.67 and −0.94 kcal/mol), respectively. TS5c and TS6c are the transition states for the addition of OH at terminal and middle carbon atoms of the ⟩C=C⟨ bond.

3.3.3. Isomerization and dissociation pathways

The ADT1c will undergo isomerization leading to ADT3c (−37.65 kcal/mol) and ADT5c (−48.76 kcal/mol) via four membered ring TS7c (−11.13 kcal/mol) by transfer of hydroxyl hydrogen to the middle carbon and TS8c (−11.69 kcal/mol) by transfer of fluorine which is attached with terminal carbon to the middle carbon, respectively. The ADT1c may undergo terminal C—F cleavage to form CF_3CF=CF (OH) + H, but this pathway is not existing and favors the formation of ADT5c. ADT3c will undergo C—C bond (which is originated from ⟩C=C⟨ bond) cleavage via TS9c (−32.49 kcal/mol) and C—F bond cleavage at terminal carbon via TS10c (−6.44 kcal/mol) to yield bi-products FCFO + CF_3•CHF (−44.81 kcal/mol) and H + $CF_3CHFCFO$ (−10.83 kcal/mol), respectively. ADT5c yields the bi-products CF_3 + CF_2=CF (OH) (−6.41 kcal/mol) via TS11c (−5.30 kcal/mol) by CF_3—C cleavage and H + CF_3CF_2CFO (−26.15 kcal/mol) via TS12c (−13.05 kcal/mol) by O—H cleavage.

ADT2c will undergo isomerization leading to ADT4c (−37.17 kcal/mol) and ADT6c (−59.21 kcal/mol) via four membered ring TS14c (−5.13 kcal/mol) by transfer of hydroxyl hydrogen to the terminal carbon and TS15c (−12.29 kcal/mol) by transfer of fluorine which is attached with middle carbon to terminal carbon, respectively. Also the ADT2c will undergo CF_3—C cleavage via TS13c (−6.02 kcal/mol) to form CF_3 + CF (OH)=CF_2 (−6.29 kcal/mol). The ADT4c will undergo (i) CHF_2—C bond cleavage via TS16c (−30.88 kcal/mol) to

yield bi-products $CF_3CFO + CHF_2$ (−34.74 kcal/mol), (ii) CF_3—C bond cleavage via TS17c (−27.83 kcal/mol) to yield bi-products $CHF_2CFO + CF_3$ (−33.3 kcal/mol) and (iii) middle C—F bond cleavage via TS18c (5.75 kcal/mol) to yield bi-products $CF_3COCHF_2 + F$ (3.39 kcal/mol), respectively. ADT6c yields the bi-products $CF_3COCF_3 + H$ (−20.3 kcal/mol) via TS19c (−11.12 kcal/mol) by O—H bond cleavage.

The energy profile for the reaction of $OH + CF_3CF{=}CF_2$ is given in SI (Fig. S-V-1c). In our mechanistic studies, the products CF_3CFO and FCFO which are formed through the lowest energy pathways are most feasible compared to the other products. Also a simplified atmospheric OH initiated degradation mechanism for $CF_3CF{=}CF_2$ in NO_x rich conditions is suggested and is shown in SI (Fig. S-V-3). (The degradation mechanisms for the other two reactions were reported in the literature.)

3.4. Rate coefficients

Dual level direct dynamic approach (M06-2X/MG3S//M06-2X/6-31+G(d,p)) was used to study the initial step in the reactions of hydroxyl radicals with $CF_3CH{=}CH_2$, $CF_3CF{=}CH_2$ and $CF_3CF{=}CF_2$. In this methodology, the reaction path information, including geometries, first derivatives, and frequencies of stationary points along the reaction path of initial step, was obtained at lower-level M06-2X/6-31+G(d,p). To improve the accuracy of barrier heights and reaction energies and few non-stationary points, we employed higher-level calculations at M06-2X/MG3S. The rate coefficients are calculated by variational transition state theory (VTST) with the interpolated single-point energies [33] (ISPE) method, developed by Truhlar et al. In the present study, single-point energies evaluated at four non-stationary points (ISPE-4) are used to correct the lower-level reaction path. The minimum energy pathway is obtained using direct dynamics for a small range of the reaction path with the mass scaled reaction coordinate '*s*' from −1.0 Å to 1.0 Å by using the Page–McIver integrator with a step size of 0.1 Å. A Hessian matrix was calculated every step. Also the harmonic frequencies were scaled by 0.979 along the reaction path. All vibrations are treated harmonically except for the lowest vibrational modes. The internal rotation modes are treated using the hindered rotor approximation, whereas the remaining vibrations are treated harmonically. The generalized rate coefficient can be minimized by varying the transition state dividing surface along the reaction coordinate to get canonical variational transition state rate coefficient using the following equations:

$$k^{GT}(T,s) = \sigma \frac{k_B T}{h} \left(\frac{Q^{GT}(T,s)}{\Phi^R(T)} \right) \exp\left(\frac{-V_{MEP}(s)}{k_B T} \right)$$

$$k^{CVT}(T) = \min_s k^{GT}(T,s) = k^{GT}[T, s^{CVT}(T)]$$

where k^{GT} and k^{CVT} are the rate coefficients of generalized and canonical variational transition state theories, respectively, σ is reaction path degeneracy, k_B is Boltzmann's constant, h is Planck's constant, T is temperature in Kelvin, s^{CVT} is the reaction coordinate (s) at which canonical variational transition state dividing surface was found. Q^{GT} and Φ^R are the partition functions of a generalized TS at '*s*' and reactants, respectively. $V_{MEP}(s)$ is the potential energy of generalized TS at '*s*'. The canonical variational transition state is located by maximizing the free energy of activation with respect to '*s*'. The tunneling corrected rate coefficients were obtained by multiplying the CVT rate constant by a temperature-dependent transmission coefficient $\kappa^{CVT/SCT}(T)$.

$$k^{CVT/SCT}(T) = \kappa^{CVT/SCT}(T) k^{CVT}(T)$$

The electronic partition function of OH radical was evaluated by taking the splitting of 140 cm^{-1} in the $^2\Pi$ ground state, into account [34].

$$Q^E(OH) = 2 + 2\exp\left[-\frac{140(cm^{-1})hc_o}{k_B T} \right]$$

where c_o is velocity of light in vacuum.

Using the above described methodology, rate coefficients for the reaction of hydroxyl radicals with $CF_3CH{=}CH_2$, $CF_3CF{=}CH_2$, and $CF_3CF{=}CF_2$ were computed in the temperature range of 200–3000 K. The total rate coefficients for the title reactions are given in Table 1. The rate coefficients for the initial addition and abstraction pathways, which were calculated by CVT/SCT/ISPE method, are given in SI (Table S-VI-1).

The variational effects for the addition reaction pathways are found to be significant. The ratios of TST and CVT for the formation of ADT1 and ADT2 in the temperature range of 200–3000 K for the reaction of OH with test molecule, are given in SI (Table S-VI-2). In case of barrier less addition pathways, the tunneling effect is insignificant throughout the studied temperature range, whereas in case of abstraction pathways, the tunneling effect is decreasing with increase in temperature.

The Arrhenius plots for the computed rate coefficients in the temperature range of 200–3000 K are compared with literature values and shown in Fig. 2. The modified Arrhenius expression (in cm^3 $molecule^{-1}$ s^{-1}) is used to fit the non linear behavior temperature dependent rate coefficients, for the reaction of OH+ $CF_3CH{=}CH_2$, $CF_3CF{=}CH_2$, and $CF_3CF{=}CF_2$ in the temperature range of 200–3000 K as given below:

$$k(1) = 1.04 \times 10^{-21} (T)^{3.02} \exp\left(\frac{1134.9}{T} \right)$$

$$k(2) = 4.01 \times 10^{-20} (T)^{2.44} \exp\left(\frac{921.26}{T} \right)$$

$$k(3) = 5.82 \times 10^{-20} (T)^{2.21} \exp\left(\frac{1378.0}{T} \right)$$

The shapes of the curves and the minima in the Arrhenius plot are due to the existence of two different competing reactions viz., addition and abstraction channels. Each channel is possessing different activation energy and each one is dominating at a particular range of temperature and therefore the overall rate coefficient is the combination of multiple channels. The rate coefficients of all the test molecules obtained by CVT/SCT/ISPE method are compared with the available literature values in the studied temperature range and are given in Table 2.

The computed rate coefficient at 298 K for the reaction of $OH + CF_3CH{=}CH_2$ is 1.48×10^{-12} cm^3 $molecule^{-1}$ s^{-1} which is in good agreement with the one reported by Sulbaek Andersen et al. [6] [$(1.36 \pm 0.25) \times 10^{-12}$ cm^3 $molecule^{-1}$ s^{-1}] within the error limits, also by Orkin et al. [3] [$(1.54 \pm 0.05) \times 10^{-12}$ cm^3 $molecule^{-1}$ s^{-1}]. The rate coefficient reported by Zhang et al. [8] [1.65×10^{-12}] is also in reasonably good agreement with our computed one at 298 K only. However, they have reported strong positive temperature dependence in their studied temperature range. Whereas, all other reports including ours have been shown negative temperature dependence. The rate coefficient at 298 K predicted (using TST/Wigner method) by Thomsen et al. [7] [4.09×10^{-12} cm^3 $molecule^{-1}$ s^{-1}] is ~3 times higher than experimental values. A completely linear behavior was observed in the experimentally measured rate coefficients by Orkin et al. [3]. However, a non linear behavior is observed in our current study. This non-linear behavior is expected because of the presence of double bond in the molecule, where addition plays a

Table 1
Calculated rate coefficients (cm^3 $molecule^{-1}$ s^{-1}) for the reaction of OH radical with $CF_3CH{=}CH_2$, $CF_3CF{=}CH_2$ and $CF_3CF{=}CF_2$ at M06-2X/MG3S//M06-2X/6-31+G(d,p) level of theory over the temperature range 200–3000 K.

Temperature (K)	Rate coefficients (cm^3 $molecule^{-1}$ s^{-1})		
	k (OH + $CF_3CH{=}CH_2$)[a]	k (OH + $CF_3CF{=}CH_2$)[b]	k (OH + $CF_3CF{=}CF_2$)[c]
200	2.16×10^{-12}	1.48×10^{-12}	6.62×10^{-12}
298	1.48×10^{-12}	1.02×10^{-12}	1.77×10^{-12}
400	1.40×10^{-12}	9.84×10^{-13}	1.03×10^{-12}
500	1.51×10^{-12}	1.04×10^{-12}	8.37×10^{-13}
600	1.70×10^{-12}	1.15×10^{-12}	7.83×10^{-13}
700	1.94×10^{-12}	1.30×10^{-12}	7.89×10^{-13}
800	2.26×10^{-12}	1.49×10^{-12}	8.27×10^{-13}
900	2.66×10^{-12}	1.70×10^{-12}	8.85×10^{-13}
1000	3.15×10^{-12}	1.96×10^{-12}	9.59×10^{-13}
1200	4.47×10^{-12}	2.60×10^{-12}	1.15×10^{-12}
1500	7.48×10^{-12}	3.90×10^{-12}	1.51×10^{-12}
1800	1.20×10^{-11}	5.70×10^{-12}	1.95×10^{-12}
2000	1.61×10^{-11}	7.24×10^{-12}	2.28×10^{-12}
2500	3.34×10^{-11}	1.24×10^{-11}	3.27×10^{-12}
3000	5.71×10^{-11}	1.96×10^{-11}	4.47×10^{-12}

[a] $k(OH + CF_3CH{=}CH_2) = k_{TS1a} + k_{TS2a} + k_{TS3a} + k_{TS5a} + k_{TS6a}$.
[b] $k(OH + CF_3CF{=}CH_2) = k_{TS1b} + k_{TS2b} + k_{TS5b} + k_{TS6b}$.
[c] $k(OH + CF_3CF{=}CF_2) = k_{TS5c} + k_{TS6c}$.

very important role. This behavior can better be explained, if the experiments are carried out in absolute methods.

In case of $CF_3CF{=}CH_2$ + OH reaction kinetics, Orkin et al. [4], Nielsen et al. [9] and Papadimitriou et al. [10] studied this reaction independently with different experimental techniques. The rate coefficients which are reported by them are in good agreement with each other, and the average rate constant is 1.10×10^{-12} cm^3 $molecule^{-1}$ s^{-1}. Du et al. [11] studied the kinetics of this reaction theoretically and computed the rate coefficients in the temperature range of 206–380 K using transition state theory with Wigner tunneling correction. They have reported the rate coefficient at 298 K to be 8.1×10^{-11} cm^3 $molecule^{-1}$ s^{-1}. Our computed rate coefficient at 298 K is 1.02×10^{-12} cm^3 $molecule^{-1}$ s^{-1}, which is in excellent agreement with the experimentally determined one and ~1.2 times higher than the one reported by Du et al. [11]. The computed rate coefficients using CVT/SCT/ISPE in the present study are in excellent agreement with the experimentally measured rate coefficients over the complete range of temperatures. The rate coefficients reported by Du et al. [11] are lower than the experimentally measured rate coefficients over the complete range of studied temperature. The deviation from the experimental values is more at lower temperatures when compared with that of higher temperatures. The non-linear behavior is seen in all the reported studies as well as in our calculations, irrespective of the agreement among these studies.

Though the reaction of OH with $CF_3CF{=}CF_2$ was studied experimentally by several research groups, no theoretical investigation is reported so far, to the best of our knowledge. Recently, Orkin

Table 2
Total rate coefficients for the addition reactions of OH radical with $CF_3CH{=}CH_2$, $CF_3CF{=}CH_2$ and $CF_3CF{=}CF_2$ at M06-2X/MG3S//M06-2X/6-31+G(d,p) level of theory at 298 K were compared with reported rate coefficient for the corresponding reactants (Arrhenius parameters are computed in the temperature range of 200–400 K, where the experimental values are available).

Reactions	Kinetic parameters[a]			Rate coefficients (10^{-12} cm^3 $molecule^{-1}$ s^{-1}) at 298 K
	A (cm^3 $molecule^{-1}$ s^{-1})	n	E_a (kcal/mol)	
$CF_3CH{=}CH_2$ + OH	1.63×10^{-17}	1.63	−1.25	1.48 (this work)[b]
	8.28×10^{-13}	0	−0.36	(1.54 ± 0.05) [3]
	–	–	–	(1.36 ± 0.25)[c] [6]
	–	–	–	4.09 [7]
	7.27×10^{-18}	1.94	−0.761	1.65 [8]
$CF_3CF{=}CH_2$ + OH	6.15×10^{-18}	1.73	−1.27	1.02 (this work)[b]
	1.41×10^{-12}	0	0.13	(1.12 ± 0.02) [3]
	4.06×10^{-13}	1.17	−0.59	(1.10 ± 0.07) [4]
	–	–	–	(1.05 ± 0.17)[c] [9]
	1.26×10^{-12}	0	0.07	(1.12 ± 0.09)[c] [10]
	1.24×10^{-12}	0	0.24	0.81[c] [11]
$CF_3CF{=}CF_2$ + OH	1.93×10^{-18}	1.69	−2.41	1.77 (this work)[b]
	9.75×10^{-14}	1.94	−1.83	(2.17 ± 0.08) [3,6]
	8.74×10^{-13}	–	−0.52	(2.12 ± 0.02) [12]
	–	–	–	(2.40 ± 0.30)[c] [13]
	–	–	–	(2.60 ± 0.70) [14]
	9.95×10^{-13}	0	−0.97	(2.26 ± 0.12)[d] [15]
	6.00×10^{-13}	0	−0.74	(2.10 ± 0.05)[c] [16]

[a] Rate expression is given by linear least square fit, if $n = 0$. Rate expression is given by three parameter fit, if $n > 0$. Blank rows correspond to the rate coefficients reported at single temperature in the literature.
[b] Rate coefficients obtained by CVT/SCT/ISPE method.
[c] Rate coefficients obtained at 296 K.
[d] Rate coefficients obtained at 293 K.

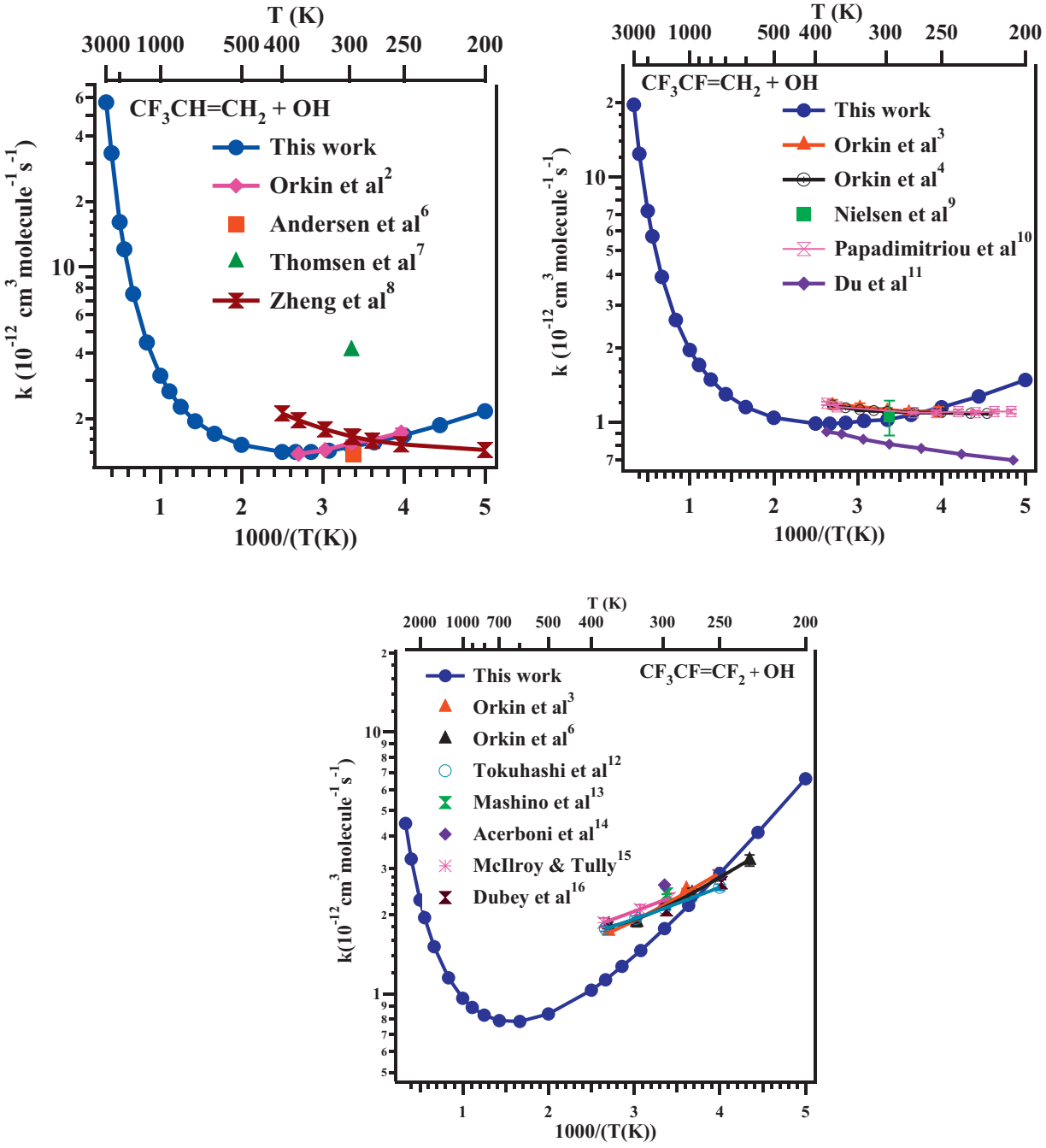

Fig. 2. Arrhenius plots for the rate coefficients data obtained from the addition reaction of OH radical with $CF_3CH{=}CH_2$, $CF_3CF{=}CH_2$ and $CF_3CF{=}CF_2$ over the temperature range of 200–3000 K.

et al. [5] studied this reaction using flash photolysis-resonance fluorescence technique between 230 and 480 K. They noticed curvature in Arrhenius plot and reported the rate coefficient in modified Arrhenius expression, which is consistent with our results. Three parameter fit was used for fitting the rate coefficients obtained in the present investigation. Though our rate coefficient [1.77×10^{-12} cm^3 molecule^{-1} s^{-1}] is 1.23 times lower than Orkin et al. [5] [2.17×10^{-12} cm^3 molecule^{-1} s^{-1}], barrier energy predicted in our calculations [−2.41 kcal/mol] is in good agreement with the one reported by Orkin et al. [5] [−1.83 kcal/mol]. But the predicted activation energies by Tokuhashi et al. [12] and Dubey et al. [16] are ~4.6 and ~3.3 times higher than the activation energy obtained in the present study. Also Tokuhashi et al. [12] [$(2.12 \pm 0.02) \times 10^{-12}$ cm^3 molecule^{-1} s^{-1}], Mashino et al. [13] [$(2.4 \pm 0.3) \times 10^{-12}$ cm^3 molecule^{-1} s^{-1}], Acerboni et al. [14] [$(2.6 \pm 0.7) \times 10^{-12}$ cm^3 molecule^{-1} s^{-1}], McIlroy and Tully [15] [$(2.26 \pm 0.12) \times 10^{-12}$ cm^3 molecule^{-1} s^{-1}] and Dubey et al. [16] [$(2.10 \pm 0.05) \times 10^{-12}$ cm^3 molecule^{-1} s^{-1}] studied the kinetics of this reaction with various experimental techniques. Since the experimentally reported rate coefficients are in good agreement between each other; we have averaged all the rate coefficients to compare with our result. The averaged rate coefficient [2.28×10^{-12} cm^3 molecule^{-1} s^{-1}] obtained from all experimental investigations is ~1.3 times higher than the rate coefficient [1.77×10^{-12} cm^3 molecule^{-1} s^{-1}] predicted in this study. All reported rate coefficients are compared with our prediction is shown in Fig. 2. Just like in case of the second reaction, the computed rate coefficients using CVT/SCT/ISPE in the present study are

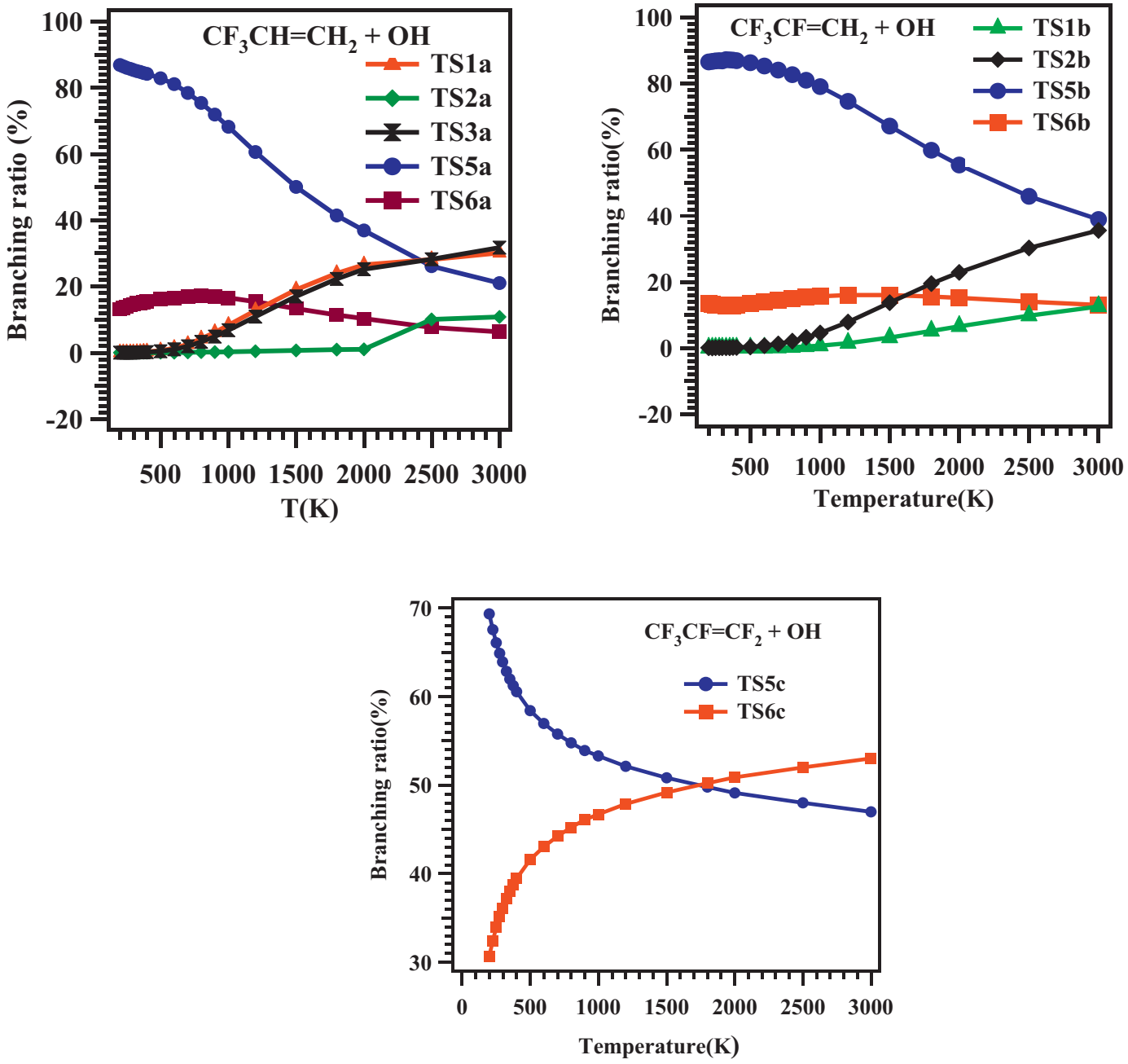

Fig. 3. Plots for the percentage contribution of H atom abstraction and addition (on middle and terminal carbon) to the total rate coefficients (= k (abstraction) + k (middle) + k (terminal)) within the temperature range of 200–3000 K.

in very good agreement with the experimentally measured rate coefficients over the complete range of temperatures.

The presence of three fluorine atoms in this molecule ($CF_3CF{=}CF_2$) makes it different from the rest of the two test molecules. The highly electro negative property of fluorine atoms makes the ⟩C=C⟨ bond more electrophilic in nature compared to the less fluorinated other two molecules. And the addition reaction is more favorable than the rest of the molecules. And therefore, this reaction is relatively faster than the other two reactions.

The calculated rate coefficients using CVT/SCT/ISPE method are reliable and used for deriving Arrhenius expression, also in determining the atmospheric lifetimes and GWPs. The rate coefficients obtained for abstraction reactions are observed to be negligible when compared to addition reactions in the lower temperature range. But in the higher temperature range, abstraction pathways are becoming dominant and contribution of these rate coefficients to the overall rate coefficient will be significant. The percentage contribution of abstraction and addition rate coefficients to the total rate (= k (abstraction) + k (addition)) are given in SI (Table S-VI-3) and shown in Fig. 3.

The conclusions of percentage contribution analysis are (i) abstraction rate coefficients are negligible at lower temperature and contribute significantly at higher temperatures, (ii) addition rate coefficients for middle carbon are low at lower temperature but increasing with increase in temperature and (iii) addition rate coefficients for terminal carbon are high but decreasing with increase in temperature. It is also apparent from the energy level diagrams shown in Fig. 1 that, pathways for the formation of adducts ADT1s and ADT2s require less energy than for the abstraction pathways.

Table 3
The atmospheric lifetimes (computed at 277 K) and global warming potentials (GWPs) of $CF_3CH{=}CH_2$, $CF_3CF{=}CH_2$ and $CF_3CF{=}CF_2$ computed for the time horizon 20, 100 and 500 years (reported values are given in parentheses).

Reactants	Life time (days) at 277 K		Total radiative forcing (w/m^2 ppbv)	GWPs (years)		
	This work	Reported values		20	100	500
$CF_3CH{=}CH_2$	8	(9) [6] (8) [31]	0.205	8.7	2.66	0.83
$CF_3CF{=}CH_2$	11	(11) [9] (12) [10] (11) [32]	0.207 (0.24) [10]	10.4 (15.6) [10]	3.19 (4.4) [10]	1.00 (1.3) [10]
$CF_3CF{=}CF_2$	6	(5) [5] (9) [13] (6) [14]	0.194 (0.28) [14]	3.16 (0.86) [14]	1.12 (0.25) [14]	0.35 (0.08) [14]

3.5. Atmospheric lifetime and global warming potential

Since hydrofluoroolefins are having zero ozone depletion potential, the atmospheric lifetime and GWP are the deciding factors to consider these compounds to be alternatives to existing CFCs and its alternatives. The reactions with hydroxyl radical in the atmosphere plays a major role in determining the compound's life time, as it is considered to be the detergent of the atmosphere and most powerful oxidizing agent. Using a global weighted-average OH concentration [35] (1×10^6 molecules cm^{-3}), we estimated the lifetimes of HFOs with respect to the reactions with OH radicals. The procedures for calculation of lifetimes and GWP [36–38] are described elsewhere in our previous article [19] and references therein. The computed atmospheric lifetimes for $CF_3CH{=}CH_2$, $CF_3CF{=}CH_2$ and $CF_3CF{=}CF_2$ are 8, 11 and 6 days, respectively, which are very low compared to CFCs and any contribution of these compounds to radiative forcing of climate change will be negligible. Therefore, their contribution to the GWPs at all the time horizons will be just negligible. Although the GWP_S are negligible, we have computed them for the purpose of comparison with the values available in the literature. The computed GWPs of the test molecules are very low (as high as 10) when compared to CFCs. The computed lifetimes compared with reported values and GWP for the different time horizons (20, 100, and 500 years) are given in Table 3. Based on the lifetimes and GWPs, all the three test molecules namely, $CF_3CF{=}CF_2$, $CF_3CH{=}CH_2$ and $CF_3CF{=}CH_2$ may be good substitutes to HFCs and CFCs in the point of view of their atmospheric lifetimes.

4. Conclusions

A detailed mechanistic study on the reactions of OH + ($CF_3CH{=}CH_2$, $CF_3CF{=}CH_2$ and $CF_3CF{=}CF_2$) are reported at M06-2X/MG3S//M06-2X/6-31+G(d,p) level of theory. In general, the reaction proceeds most likely through OH attacking at the unsaturated ⟩C=C⟨ bond leading to adducts ADT1 and ADT2 with small positive barriers or negative barriers and abstraction reactions. Dual level dynamic calculations were carried out using CVT/SCT/ISPE approach to calculate the total rate coefficients for the title reactions in the temperature range of 200–3000 K and they are in good agreement with reported values. The addition reactions are dominant and the abstraction reactions are negligible at below 500 K, however abstraction reactions become competitive when temperature increases. Non-linear behavior in the kinetic behavior is observed due to the presence of double bond in the test molecules. The calculated atmospheric lifetimes and global warming potential values suggest that $CF_3CF{=}CF_2$, $CF_3CH{=}CH_2$ and $CF_3CF{=}CH_2$ may be considered as good replacement compounds as HFCs and CFCs.

Acknowledgments

The authors thank Professor D.G. Truhlar for providing the POLYRATE 2008 and GAUSSRATE 2009A programs. Also the authors thank the High Performance Computing Service and Mr. V. Ravichandran for providing computer resources.

Appendix A. Supplementary data

Supplementary data associated with this article can be found, in the online version, at http://dx.doi.org/10.1016/j.jmgm.2013.12.003.

References

[1] M.J. Molina, F.S. Rowland, Stratospheric sink for chlorofluoromethanes: chlorine atom-catalysed destruction of ozone, Nature 249 (1974) 810–812.
[2] A.R. Ravishankara, S. Solomon, A.A. Turnipseed, R.F. Warren, Atmospheric lifetimes of long-lived halogenated species, Science 259 (1993) 194–199.
[3] V.L. Orkin, R.E. Huie, M.J. Kurylo, Rate constants for the reactions of OH with HFC-245cb ($CH_3CF_2CF_3$) and some fluoroalkenes (CH_2CHCF_3, CH_2CFCF_3, CF_2CFCF_3, and CF_2CF_2), J. Phys. Chem. A 101 (1997) 9118–9124.
[4] V.L. Orkin, L.E. Martynova, A.N. Ilichev, High-accuracy measurements of OH reaction rate constants and IR absorption spectra: $CH_2{=}CF{-}CF_3$ and trans-$CHF{=}CH{-}CF_3$, J. Phys. Chem. A 114 (2010) 5967–5979.
[5] V.L. Orkin, G.A. Poskrebyshev, M.J. Kurylo, Rate constants for the reactions between OH and perfluorinated alkenes, J. Phys. Chem. A 115 (2011) 6568–6574.
[6] M.P. Sulbaek Andersen, O.J. Nielsen, A. Toft, T. Nakayama, Y. Matsumi, R.L. Waterland, R.C. Buck, M.D. Hurley, T.J. Wallington, Atmospheric chemistry of $C_xF_{2x+1}CH{=}CH_2$ (x = 1, 2, 4, 6, and 8): kinetics of gas-phase reactions with Cl atoms, OH radicals, and O_3, J. Photochem. Photobiol. A: Chem. 176 (2005) 124–128.
[7] D.L. Thomsen, S.A. Jorgensen, Theoretical study of the kinetics of OH radical addition to halogen substituted propenes, Chem. Phys. Lett. 481 (2009) 29–33.
[8] Y. Zhang, J. Sun, K. Chao, H. Sun, F. Wang, S. Tang, X. Pan, J. Zhang, R. Wang, Mechanistic and kinetic study of $CF_3CH{=}CH_2$ + OH reaction, J. Phys. Chem. A 116 (2012) 3172–3181.
[9] O.J. Nielsen, M.S. Javadi, M.P. Sulbaek Andersen, M.D. Hurley, T.J. Wallington, R. Singh, Atmospheric chemistry of $CF_3CF{=}CH_2$: kinetics and mechanisms of gas-phase reactions with Cl atoms, OH radicals, and O_3, Chem. Phys. Lett. 439 (2007) 18–22.
[10] V.C. Papadimitriou, R.K. Talukdar, R.W. Portmann, A.R. Ravishankara, J.B. Burkholder, $CF_3CF{=}CH_2$ and (Z)-$CF_3CF{=}CHF$: temperature dependent OH rate coefficients and global warming potentials, Phys. Chem. Chem. Phys. 10 (2008) 808–820.
[11] B. Du, C. Feng, W. Zhang, Theoretical studies on the reaction mechanisms and rate constants for OH radicals with $CF_3CF{=}CH_2$, Chem. Phys. Lett. 479 (2009) 37–42.
[12] K. Tokuhashi, A. Takahashi, M. Kaise, S. Kondo, A. Sekiya, E. Fujimoto, Rate constants for the reactions of OH radicals with $CF_3OCF{=}CF_2$ and $CF_3CF{=}CF_2$, Chem. Phys. Lett. 325 (2000) 189–195.
[13] M. Mashino, Y. Ninomiya, M. Kawasaki, T.J. Wallington, M.D. Hurley, Atmospheric chemistry of $CF_3CF{=}CF_2$: kinetics and mechanism of its reactions with OH radicals, Cl atoms, and ozone, J. Phys. Chem. A 104 (2000) 7255–7260.
[14] G. Acerboni, J.A. Beukes, N.R. Jensen, J. Hjorth, G. Myhre, C.J. Nielsen, J.K. Sundet, Atmospheric degradation and global warming potentials of three perfluoroalkenes, Atmos. Environ. 35 (2001) 4113–4123.
[15] A. McIlroy, F.P. Tully, Kinetic study of OH reactions with perfluoropropene and perfluorobenzene, J. Phys. Chem. 97 (1993) 610–614.

[16] M.K. Dubey, T.F. Hanisco, P.O. Wennberg, J.G. Anderson, Monitoring potential photochemical interference in laserinduced fluorescence measurements of atmospheric OH, Geophys. Res. Lett. 23 (1996) 3215–3218.
[17] Y. Zhao, D.G. Truhlar, The M06 suite of density functionals for main group thermochemistry, thermochemical kinetics, noncovalent interactions, excited states, and transition elements: two new functionals and systematic testing of four M06 functionals and twelve other functionals, Theor. Chem. Acc. 120 (2008) 215–241.
[18] Y. Zhao, D.G. Truhlar, Density functionals with broad applicability in chemistry, Acc. Chem. Res. 41 (2008) 157–167.
[19] M. Balaganesh, B. Rajakumar, Rate coefficients and reaction mechanism for the reaction of OH radicals with (*E*)-$CF_3CH{=}CHF$, (*Z*)-$CF_3CH{=}CHF$, (*E*)-$CF_3CF{=}CHF$, and (*Z*)-$CF_3CF{=}CHF$ between 200 and 400 K: hybrid density functional theory and canonical variational transition state theory calculations, J. Phys. Chem. A 116 (2012) 9832–9842.
[20] C. Gonzalez, H.B. Schlegel, An improved algorithm for reaction path following, J. Chem. Phys. 90 (1989) 2154–2161.
[21] I.M. Alecu, J. Zheng, Y. Zhao, D.G. Truhlar, Computational thermochemistry scale factor databases and scale factors for vibrational frequencies obtained from electronic model chemistries, J. Chem. Theory Comput. 6 (2010) 2872–2887.
[22] A. Gonzalez-Lafont, T.N. Truong, D.G. Truhlar, Interpolated variational transition-state theory: practical methods for estimating variational transition-state properties and tunneling contributions to chemical reaction rates from electronic structure calculations, J. Chem. Phys. 95 (1991) 8875–8894.
[23] B.C. Garrett, D.G. Truhlar, Generalized transition state theory. Classical mechanical theory and applications to collinear reactions of hydrogen molecules, J. Phys. Chem. 83 (1979) 1052–1079.
[24] B.C. Garrett, D.G. Truhlar, R.S. Grev, A.W. Magnuson, Improved treatment of threshold contributions in variational transition-state theory, J. Phys. Chem. 84 (1980) 1730–1748.
[25] D.H. Lu, T.N. Truong, V.S. Melissas, G.C. Lynch, Y.P. Liu, B.C. Garrett, R. Steckler, A.D. Isaacson, S.N. Rai, G.C. Hancock, POLYRATE 4: a new version of a computer program for the calculation of chemical reaction rates for polyatomics, Comput. Phys. Commun. 71 (1992) 235–262.
[26] Y.P. Liu, G.C. Lynch, T.N. Truong, D.H. Lu, D.G. Truhlar, B.C. Garrett, Molecular modeling of the kinetic isotope effect for the [1,5]-sigmatropic rearrangement of cis-1,3-pentadiene, J. Am. Chem. Soc. 115 (1993) 2408–2415.
[27] J. Zheng, S. Zhang, B.J. Lynch, J.C. Corchado, Y.-Y. Chuang, P.L. Fast, W.-P. Hu, Y.-P. Liu, G.C. Lynch, K.A. Nguyen, et al., POLYRATE – Version 2008, University of Minnesota, Minneapolis, MN, 2009.
[28] J. Zheng, S. Zhang, J.C. Corchado, Y.-Y. Chuang, E.L. Coitiño, B.A. Ellingson, D.G. Truhlar, GAUSSRATE – Version 2009-A, University of Minnesota, Minneapolis, MN, 2010.
[29] M.J. Frisch, G.W. Trucks, H.B. Schlegel, G.E. Scuseria, M.A. Robb, J.R. Cheeseman, G. Scalmani, V. Barone, B. Mennucci, G.A. Petersson, et al., Gaussian 09, Revision B.01, Gaussian, Inc., Wallingford, CT, 2010.
[30] I.I.R. Dennington, T. Keith, J. Millam, K. Eppinnett, W.L. Hovell, R. Gilliland, GaussView, Version 3.09, Semichem, Inc., Shawnee Mission, KS, 2003.
[31] T. Nakayama, K. Takahashi, Y. Matsumi, A. Toft, M.P. Sulbaek Andersen, O.J. Nielsen, R.L. Waterland, R.C. Buck, M.D. Hurley, T.J. Wallington, Atmospheric chemistry of $CF_3CH{=}CH_2$ and $C_4F_9CH{=}CH_2$: products of the gas-phase reactions with Cl atoms and OH radicals, J. Phys. Chem. A 111 (2007) 909–915.
[32] M.D. Hurley, T.J. Wallington, M.S. Javadi, O.J. Nielsen, Atmospheric chemistry of $CF_3CF{=}CH_2$: products and mechanisms of Cl atom and OH radical initiated oxidation, Chem. Phys. Lett. 450 (2008) 263–267.
[33] Y.-Y. Chuang, J.C. Corchado, D.G. Truhlar, Mapped interpolation scheme for single-point energy corrections in reaction rate calculations and a critical evaluation of dual-level reaction path dynamics methods, J. Phys. Chem. 103 (1999) 1140–1149.
[34] M.W. Chase Jr., NIST-JANAF Thermo Chemical Tables, J. Phys. Chem. Ref. Data, fourth ed., 1998, pp. 1 (Monograph No. 9).
[35] R.G. Prinn, J. Huang, R.F. Weiss, D.M. Cunnold, P.J. Fraser, P.G. Simmonds, A. McCulloch, P. Salameh, S. O'Doherty, R.H.J. Wang, L. Porter, B.R. Miller, Evidence for substantial variations of atmospheric hydroxyl radicals in the past two decades, Science 292 (2001) 1882–1888.
[36] P. Blowers, D.M. Moline, K.F. Tetrault, R.R. Wheeler, S.L. Tuchawena, Prediction of radiative forcing values for hydrofluoroethers using density functional theory methods, J. Geophys. Res. Atmos. 112 (2007) D15108.
[37] P. Blowers, D.M. Moline, K.F. Tetrault, R.R. Wheeler, S.L. Tuchawena, Global warming potentials of hydrofluoroethers, Environ. Sci. Technol. 42 (2008) 1301–1307.
[38] S. Pinnock, M.D. Hurley, K.P. Shine, T.J. Wallington, T.J. Smyth, Radiative forcing of climate by hydrochlorofluorocarbons and hydrofluorocarbons, J. Geophys. Res. Atmos. 100 (1995) 23227–23238.